Journal of Proteomics & Bioinformatics - Open Access

Research Article
OPEN ACCESS Freely available online
doi:10.4172/jpb.1000128

JPB/Vol.3 Issue 4

Molecular Basis of Chemical Chaperone Effects of N-octyl-β-valienamine on Human β-glucosidase in Low/neutral pH Conditions

Hiroyuki Jo[1], Katsuyuki Yugi[1], Seiichiro Ogawa[1], Yoshiyuki Suzuki[2] and Yasubumi Sakakibara[1]*

[1]Department of Biosciences and Informatics, Faculty of Science and Technology, Keio University, 3-14-1 Hiyoshi, Kohoku-ku, Yokohama 223-8522, Japan
[2]International University of Health and Welfare Graduate School, 2600-1 Kita Kanemaru, Otawara 324-8501, Japan

Abstract

Chemical chaperone therapy is a strategy for restoring the activities of mutant lysosomal hydrolases. This therapy involves chemical compounds binding to the dysfunctional enzymes. The chemical chaperones for lysosomal hydrolases are anticipated to stabilize folding of target enzymes by binding at neutral pH and rescuing enzyme activities by dissociation in acidic conditions after transport to lysosome. However, the molecular basis describing the mechanism of action of chemical chaperones has not been analysed sufficiently. Here we present results derived from molecular dynamics simulations showing that the binding free energy between human β-glucosidase and its known chemical chaperone, N-octyl-β-valienamine (NOV), is lower at pH 7 than at pH 5. This observation is consistent with the hypothetical activity of chemical chaperones. The pH conditions were represented as differences in the protonation states of ionizable residues which were determined from predicted pKa values. The binding free energy change is negatively correlated to the number of hydrogen bonds (H-bonds) formed between GLU235, the acid/base catalyst of the enzyme, and the N atom of NOV. At pH 7, NOV is inserted further into the active site than at pH 5. Consequently, this provides an increase in the number of H-bonds formed. Thus, we conclude that the dissociation of NOV from β-glucosidase at pH 5 occurs due to an increase in the binding free energy change caused by protonation of several residues which decreases the number of H-bonds formed between NOV and the enzyme.

Keywords: Molecular dynamics; Binding free energy change; Hydrogen bonds; Human β-glucosidase; Chemical chaperone; *N*-octyl-β-valienamine (NOV); pKa

Introduction

Dysfunctional lysosomal hydrolases activities trigger accumulation of waste products that consequently lead to a variety of severe human diseases. For example, Fabry disease (OMIM: 301500), G_{M1}-gangliosidosis (OMIM: 230500) and Gaucher disease (OMIM: 230800) are caused by deficiencies of α-galactosidase A (Davies et al., 1996; Okumiya et al., 1995a), β-galactosidase (Boustany et al., 1993) and β-glucosidase(Amaral et al., 2000), respectively. In particular, single mutations of β-glucosidase, which catalyzes the cleavage of the β-glucoside bond of sugar chains under acidic conditions in the lysosome, can lead to the accumulation of glucosylceramide (Figure 1A) (Suzuki, 2006; Suzuki, 2008; Suzuki et al., 2007). Although some of these mutant enzymes do not lose their activity completely, the proteins are degraded and hence fail to be transported into the lysosome. As such, the absence of β-glucosidases in the lysosome is considered to be the dominant reason for the accumulation of glycolipids rather than a decrease in catalytic activity of the enzyme.

In 1995, Okumiya et al. reported that galactose restores mutant α-galactosidase activity (Okumiya et al., 1995b). Subsequently, Fan et al. (1999) discovered a paradoxical phenomenon that 1-deoxygalactonojirimycin, an inhibitor of α-galactosidase A, restores intracellular activity of mutant α-galactosidase A in cultured lymphoblasts from human patients and in transgenic mouse tissues expressing the mutant enzyme (Fan et al., 1999). Furthermore, Lin et al. (2004) reported that *N*-octyl-b-valienamine (NOV, Figure 1B), an inhibitor of β-glucosidase, exhibits similar effects on the intracellular activity of β-glucosidase (Lin et al., 2004).

The molecular mechanism describing how enzyme activity is restored by these inhibitors was proposed as follows: (Matsuda et al., 2003; Yam et al., 2005) (1) mutant enzymes are degraded in the cytoplasm because they are unstable at neutral pH, (2) binding of certain inhibitors in the ER/Golgi compartment provides stabilization of the misfolded mutant enzymes which consequently allows transport of the enzymes to the lysosome without degradation, and (3) dissociation of the inhibitors from the mutant enzymes rescues intra-lysosomal activity, thereby clearing accumulated glycolipids. These inhibitors are termed "chemical chaperones" because they stabilize proteins in a similar manner to chaperone proteins (Leandro and Gomes, 2008; Perlmutter, 2002).

However, there is insufficient information detailing the paradoxical role of the chemical chaperones: the enzyme activity in the lysosome is restored by strong inhibitors. Consequently, the detailed mechanism of action of chemical chaperones remains poorly understood.

Here we show the mechanism of restoring action of NOV on human β-glucosidase using molecular dynamics (MD) simulations. Initially, a plausible conformation of the β-glucosidase-NOV complex was predicted using a docking routine. The conformation was subjected to further structural

***Corresponding author:** Yasubumi Sakakibara, Department of Biosciences and Informatics, Faculty of Science and Technology, Keio University, 3-14-1 Hiyoshi, Kohoku-ku, Yokohama 223-8522, Japan, E-mail: yasu@bio.keio.ac.jp

Received February 10, 2010; **Accepted** March 22, 2010; **Published** March 22, 2010

Citation: Jo H, Yugi K, Ogawa S, Suzuki Y, Sakakibara Y (2010) Molecular Basis of Chemical Chaperone Effects of N-octyl-β-valienamine on Human β-glucosidase in Low/neutral pH Conditions. J Proteomics Bioinform 3: 104-112. doi:10.4172/jpb.1000128

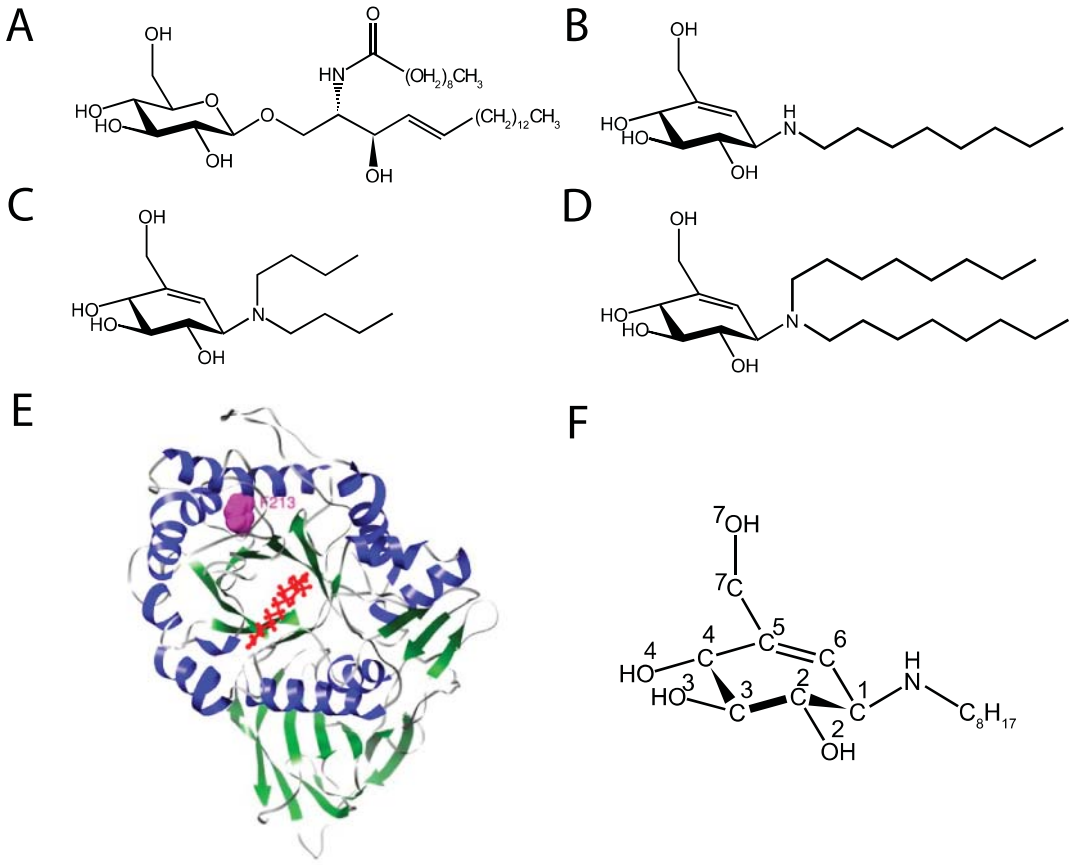

Figure 1: The structures of glycosylceramide and the chemical compounds docked to β-glucosidase in this study. (A) glycosylceramide, (B) *N*-octyl-β-valienamine (NOV), (C) *N*, *N*-dibutyl-β-valienamine (NNBV), (D) *N*, *N*-dioctyl-β-valienamine (NNOV), and (E) the complex of NOV (red) and β-glucosidase. Colored in magenta is F213 residue analyzed in later sections. Numbering of atoms of NOV are shown in (F).

optimization. The free energy changes of β-glucosidase by binding of NOV were calculated both at pH 5 and 7 using the Molecular Mechanics Poisson-Boltzmann Surface Area (MM/PBSA) method (Swanson et al., 2004) implemented in the AMBER9 package (Case et al., 2006). For the MD simulations, the pH 5 and 7 conditions were modeled by varying the protonation states of ionizable residues estimated by PROPKA (Bas et al., 2008; Li et al., 2005). The ΔG of the complex at pH 5 was calculated to be higher than the ΔG value at pH 7. At pH 7, NOV was found to be inserted deeper into the active pocket cavity than at pH 5. The nitrogen atom in the carbon chain of NOV was found to possibly provide the pH-dependent change in binding affinity. The results are consistent with the hypothesis describing the mechanism of restoring action of the chemical chaperone in which NOV dissociates from the enzyme in the acidic environment of the lysosome.

Materials and Methods

Preparation of structural data

The tertiary structure of NOV was generated using ChemDraw and Chem3D (CambridgeSoft Co.) using the first report of its chemical synthesis (Ogawa et al., 1996). Structure optimization was performed using the MM2 force field in Chem3D. Similarly, the structure of *N*, *N*-dibutyl-β-valienamine (NNBV, Figure 1C) was also prepared as a homolog of *N*, *N*-dioctyl-β-valienamine (NNOV, Figure 1D). NNOV has been reported to be an inhibitor of β-galactosidase without chemical chaperone activity(Lei et al., 2007; Ogawa et al., 1998). Since an MD simulation of the NNOV-enzyme complex provided a distorted NNOV structure (data not shown), NNBV was employed as an alternative ligand. The atomic composition of NNBV is equivalent to NOV. The optimized structure of NOV was superimposed upon the structure of 5-hydroxymethyl-3,4-dihydroxypiperidine (isofagomine, IFM) in the structure of the human β-glucosidase-IFM complex (PDBID: 2nsx) (Lieberman et al., 2007). Following the superimposition, the conformations of the carbon chains of NOV and NNBV were manually adjusted in the binding site to decrease steric hindrances. These conformations were employed as a complex structure of human β-glucosidase and either NOV or NNBV (Figure 1E).

The ionizable residues were protonated according to the pKa value of each residue predicted by PROPKA (Bas et al., 2008; Li et al., 2005) to represent pH 5 and 7 conditions. For example, an ionizable residue in the pH 5 condition was protonated if the predicted pKa of the residue was larger than 5. Otherwise, the deprotonated form was employed.

Molecular dynamics simulation

The force field for NOV and NNBV was generated using the Antechamber module of the AmberTools software suite using

Research Article
OPEN ACCESS Freely available online
doi:10.4172/jpb.1000128
JPB/Vol.3 Issue 4

the BCC charge model (Case et al., 2005). The generated force field was employed for subsequent molecular dynamics (MD) simulations of the β-glucosidase-NOV complex in combination with the AMBER99-SB force field (FF99SB) and the General AMBER force field (GAFF) in the AMBER9 package.

Optimizations and production MD simulations of the complex were conducted using the AMBER9 package. FF99 was employed for the force field of the β-glucosidase enzyme models, whereas the force field for NOV and NNBV was generated from GAFF by the Antechamber module of the AMBER9 package. TIP3P explicit water molecules and counter sodium ions were added to the environment. Distances between the enzyme and edges of the box of the periodic boundary conditions were set at 10 Å. The cutoff distances of the van der Waals interactions were 8 Å. The Particle Mesh Ewald method (Essmann et al., 1995) was employed for electrostatic interactions.

Under these conditions, five steps of MD simulations were performed: (1) energy minimization of water, (2) energy minimization of the whole system, (3) adjustment of the temperature (300 K), (4) adjustment of the pressure (1 atm) and (5) production of 3 ns of MD simulations.

In all MD simulations, the time step was 2 fs and the SHAKE algorithm (Ryckaert et al., 1977) was applied. Production MD was performed in the NPT condition. The temperature and the pressure were maintained at 300 K and 1 atm, respectively.

Calculation of the binding free energy change

The obtained MD trajectory was used to calculate the binding free energy change using the MM/PBSA method (Swanson et al., 2004) implemented in the AMBER9 package (Case et al., 2006). The representative values of the binding free energy changes shown in "Results" section are averages of those calculated from snapshots obtained every 10ns. In MM/PBSA, the binding free energy change ΔG_{bind} is defined as follows:

$$\Delta G_{bind} = G^C - G^P - G^L$$

where G^C, G^P and G^L are the free energies of the complex, protein (human β-glucosidase) and ligand, respectively. Each term (denoted G^X below) is calculated using the following formula,

$$G^X = E_{MM} + G_p + G_{np} + TS_{MM}$$

where E_{MM} is the molecular mechanical energy, G_p is the polar part of the solvation free energy calculated with a numerical solution of the Poisson-Bolzmann equation, Gnp is the non-polar part of the solvation free energy calculated with a linear model dependent on the surface area and TS_{MM} is the solute entropy term. The linear model for G_{np} is defined as the following formula:

$$G_{np} = a\,S + b$$

where S is the solvent-accessible surface area, and a and b are parameters. The default settings of a and b in AMBER9 (a=0.0072, b=0.0) were employed. The contribution from the solute entropy term TS_{MM} was ignored in this study.

Analysis of the complex structure in equilibrium

Several structural characteristics of the docked ligand were evaluated using the equilibrated enzyme-ligand complex structure. In this study, the depth of the docked ligand in the active site and the number of hydrogen bonds (H-bonds) between the enzyme and the ligand were measured. The depth of insertion of the ligand into the active site was measured by the distances between the delta carbon of active residues (GLU235 and GLU340) and seven atoms of NOV. GLU235 and GLU340 have been identified as the acid/base catalyst and the nucleophile, respectively (Fabrega et al., 2000; Miao et al., 1994; Premkumar et al., 2005). The formation of an H-bond between the donor and acceptor atoms was judged to exist when the distance between the donor-acceptor pair was ≤ 3.0 Å and the H-bond dihedral angle was ≥ 120° for at least 20% occupancy of the total simulation period. The criterion of occupancy was determined after examining previous works considering stability of H-bonds using MD simulations, for example a study presenting 50 ps of H-bond duration as the stability criterion(Kieseritzky et al., 2006) and another one which termed less than 10% occupancy as weak H-bonds

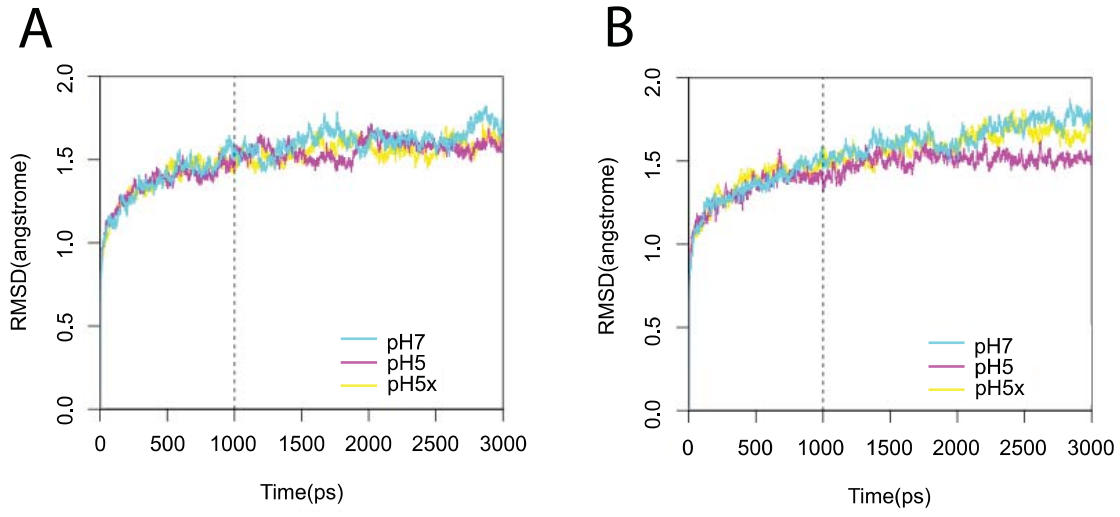

Figure 2: RMSD of the production MD of (A) the β-glucosidase-NOV complex and (B) the enzyme-NNBV complex at equilibrium. The trajectories over the period of 1-3 ns were employed to calculate the binding free energy changes.

(Rodziewicz-Motowidlo et al., 2006). In this study, we adopted 20% occupancy as the criterion of H-bond because it was appropriate to exclude trivial donor-acceptor pairs, which emerge when comparatively looser criteria such as 50 ps of duration are employed.

Protonation and conformation of NOV

Further MD simulations were performed on three structural states of NOV whose nitrogen atoms were in different protonation states (Figure 2). This approach was used to evaluate the binding free energy contribution of the H-bond between GLU235 and the N atom of NOV. This additional experiment was motivated by (1) The N atom of NOV corresponds to the glycosyl oxygen atom of glucosylceramide with which GLU235 forms an H-bond during the hydrolytic cleavage process of β-glucosidase, and (2) the equilibrium conformation of NOV indicates a correlation between the number of H-bonds on the N atom of NOV and the binding free energy change (See "Results" for details). With respect to the N atom of NOV, three conformations are possible in the solvent: R- (Figure 2A) and S-conformations (Figure2B), the lone-pair electron orbitals being oriented syn and gauche to the cyclohexene rings, respectively, and the protonated conformation (Figure 2C). The protonated structure of NOV is abbreviated NOV (P) throughout this paper. These three conformations were subjected to MD simulations and energy calculations by MM/PBSA to evaluate the correlation between the binding free energy change and an H-bond connecting the N atom of NOV and GLU235.

Analysis of F213I mutant structure

Effects of NOV on the mutant β-glucosidase were analyzed using the F213I mutation (See Figure 1E for the location of F213 residue). F213I is one of the mutations on which NOV exhibits significant diagnostic effects (Lin et al., 2004). The single residue mutation was incorporated in the wild-type structure using the UCSF Chimera (Pettersen et al., 2004). Protonation was performed according to a prediction result of PROPKA.

Residue	pKa	pH7	pH5
ASP127	5.7	-	+
ASP380	7.14	+	+
GLU233	9.28	+	+
GLU340	5.24	-	+
GLU481	5.06	-	+
HIS60	6.25	-	+
HIS145	6.5	-	+
HIS162	7.34	+	+
HIS223	6.43	-	+
HIS274	6.43	-	+
HIS290	6.43	-	+
HIS328	6.43	-	+
HIS311	7.49	+	+
HIS495	6.5	-	+
NOV	8.69	+	+

Table 1: Predicted pKa values and protonation states of ionizble residues and NOV (+: protonated). Aspartic acid, glutamic acid and histidine residues which are protonated at pH 5 are shown.

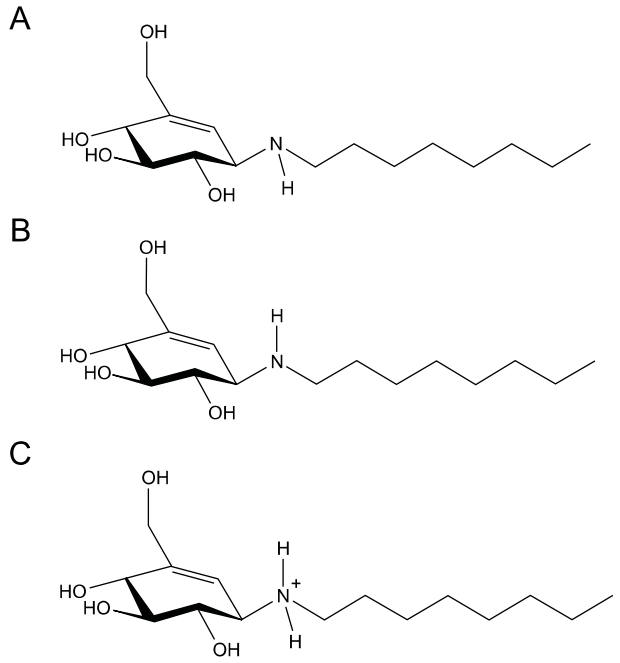

Figure 3: The three possible protonation states of the nitrogen atom of NOV in solvent. (A) The R configuration, (B) the S configuration and (C) the protonated state.

MD simulations and energy calculations were conducted on the obtained structure of the F213I mutant complex using the same procedures presented above.

Results

Protonation

The predicted pKa values by PROPKA provided protonation of ionizable residues at pH 5 and 7. With respect to aspartic acid, glutamic acid and histidine residues, 14 residues and 4 residues were protonated at pH 5 and 7, respectively (Table 1). The prediction suggested deprotonation of the proton donor GLU235 and protonation of the nucleophilic group GLU340. Since this prediction contradicts generally considered protonation states of active residues, another structure was prepared in which GLU235 was deprotonated and GLU340 was protonated. This structure is termed "pH 5X", whereas the other structures reflecting the PROPKA predictions are called "pH 7" and "pH 5". The protonation state of pH 5X is same as pH 5 except for GLU235 and GLU340. Regardless of the protonation state of residues in the pH 5 or 5X structures, the proton donor residue was deprotonated at pH 7.

MD simulations and energy calculations

Structural optimization and subsequent MD simulations were performed on six complexes: three structures (pH 7, 5 and 5X) bound by either NOV or NNBV. The RMSDs of the complexes reached a plateau after 1 ns of simulations (Figure 3).

The obtained structures demonstrated that NOV inserts more deeply into the active site of β-glucosidase at pH 7 than at either pH 5 or 5X (Figure 4A). This was corroborated by the distances between delta carbon atoms of the active residues

Research Article
OPEN ACCESS Freely available online
doi:10.4172/jpb.1000128
JPB/Vol.3 Issue 4

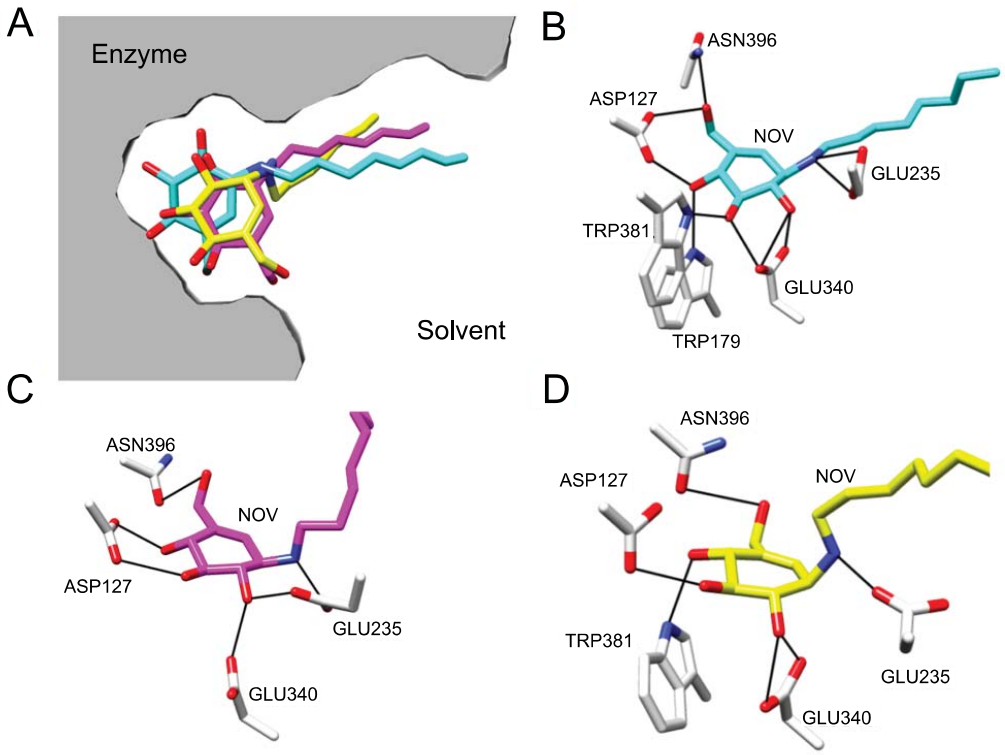

Figure 4: Configurations of NOV bound in the active site. (A) Superposed average structures of NOV (cyan: pH 7, magenta: pH 5, yellow: pH 5X). The enzyme structure is the average structure of β-glucosidase at pH 7. (B-D) H-bonds between the enzyme and NOV at pH 7, 5 and 5X, respectively.

Atom1	Atom2	Distance		
		pH7	pH5	pH5X
GLU235 CD	NOV N	3.182±0.104	3.309±0.135	3.814±0.125
GLU235 CD	NOV C1	4.118±0.133	4.152±0.109	4.694±0.166
GLU235 CD	NOV C2	3.786±0.176	3.986±0.149	4.954±0.214
GLU235 CD	NOV C3	5.357±0.187	5.432±0.153	6.436±0.206
GLU235 CD	NOV C4	6.254±0.193	6.494±0.174	7.362±0.206
GLU235 CD	NOV C5	6.226±0.169	6.440±0.114	7.167±0.165
GLU235 CD	NOV C6	5.364±0.143	5.505±0.105	6.067±0.160
GLU340 CD	NOV N	5.430±0.197	6.152±0.248	5.461±0.240
GLU340 CD	NOV C1	4.486±0.174	5.478±0.258	4.388±0.241
GLU340 CD	NOV C2	3.947±0.114	4.768±0.209	4.095±0.154
GLU340 CD	NOV C3	3.691±0.144	4.837±0.305	4.092±0.200
GLU340 CD	NOV C4	5.119±0.151	6.301±0.327	5.412±0.211
GLU340 CD	NOV C5	5.760±0.166	7.021±0.318	5.626±0.320
GLU340 CD	NOV C6	5.516±0.185	6.697±0.298	5.211±0.354

Table 2: Interatomic distances of NOV and the active site residues at three different pH values (mean ± S.D. Å). The distances at pH 7 were measured to be smaller than at the lower pH values reflecting deeper insertion of the ligand in Figure 4A. See Figure 1F for the nomenclature of the constituent atoms of NOV.

and the C1-6 atoms of NOV (Table 2). Figure 1F provides the nomenclature of the constituent atoms of NOV.

Due to the different binding depths, particular differences were observed in the H-bonds between NOV and the two residues, ASP127 and GLU235. At pH 7, ASP127 formed two stable H-bonds (occupancy > 99%) with NOV via the two oxygen atoms O4 and O5 (Figure 4B and Table 3), whereas H-bonds were formed between ASP127 and other oxygen atoms, O3 and O4, at pH 5 and 5X (Figure 4C and D, respectively). The two oxygen atoms of the GLU235 side-chain formed H-bonds with the nitrogen atom of NOV at pH 7 (Figure 4B and Table 3). At pH 5 and 5X, only one H-bond was observed between GLU235 and the N atom (Figure 4C, D and Table 3). GLU235 was found to form a second H-bond with the O2 atom of NOV at pH 5 (Table 3 and Table 4).

The binding free energy change between β-glucosidase and NOV at pH 7 was lower than the values calculated at pH 5 and 5X. In contrast, NNBV's binding free energy change at pH 7 was almost unchanged in comparison with the values at pH 5, and was higher than the value at pH 5X (Table 5). The binding free energy changes of β-glucosidase and NOV (P) were $\Delta G = -46.26$ kcal/mol at pH 7, -14.46 kcal/mol at pH 5 and -9.62 kcal/mol at pH 5X. The energy calculations by the MM/PBSA module in AMBER9 were conducted using a trajectory of 1.0-3.0 ns.

Atom(NOV)	pH7			Angle(degree)
	Residue	Occupancy (%)	Distance(Å)	
N	GLU235	22.2	2.761±0.10	48.77±9.29
N	GLU235	86.05	2.826±0.09	17.34±10.25
O2	GLU340	21.6	2.893±0.08	48.17±9.00
O2	GLU340	99.9	2.567±0.08	14.74±8.77
O3	TRP179	31.9	2.906±0.06	33.89±8.89
O3	GLU340	55.6	2.813±0.11	16.96±7.82
O4	TRP381	41.75	2.895±0.07	35.60±10.46
O4	ASP127	99.35	2.642±0.10	13.03±7.19
O5	ASN396	35.95	2.890±0.07	20.65±12.66
O5	ASP127	99.15	2.596±0.09	15.96±8.90
Atom(NOV)	pH5			Angle(degree)
	Residue	Occupancy (%)	Distance(Å)	
N	GLU235	94.55	2.796±0.08	15.24±7.96
O2	GLU340	89.15	2.747±0.10	33.25±12.33
O2	GLU235	100	2.533±0.07	11.92±6.51
O3	ASP127	27.3	2.798±0.11	16.17±9.41
O3	ASP127	47.7	2.798±0.11	23.04±11.68
O4	ASP127	65.45	2.721±0.10	14.85±8.39
O4	ASN396	26.75	2.691±0.11	16.17±9.42
O5	ASN396	16.15	2.715±0.12	19.36±11.51
Atom(NOV)	pH5X			Angle(degree)
	Residue	Occupancy (%)	Distance(Å)	
N	GLU235	95.25	2.793±0.09	17.61±9.07
O2	GLU340	24.1	2.833±0.13	35.79±14.04
O2	GLU340	93.85	2.639±0.11	18.34±10.24
O3	ASP127	86.15	2.757±0.11	14.20±7.83
O4	TRP381	34.35	2.896±0.07	32.78±11.49
O4	ASN396	96.7	2.704±0.11	17.69±9.14
O5	ASN396	49.85	2.886±0.07	21.07±10.67

Table 3: Distances and angles between the atoms of NOV and the active residues considered to form H-bonds (mean ± S.D. Å and degree, respectively). Occupancy percentage is the duration of a H-bond over simulation time. The atom-residue pairs of occupancy > 10% are presented here.

Protonation	Ligand	H-bond of NOV-GLU235		ΔG
		Possible	Observed	
pH7	NOV(P)	2	2	-46.26
pH7	NOV(R)	1	1	-24.31
pH7	NOV(S)	1	1	-27.01
pH5X	NOV(P)	1	1	-9.62
pH5X	NOV(R)	2	1	-13.45
pH5X	NOV(S)	2	1	-21.73

Table 4: Number of H-bonds formed between GLU235 and the nitrogen atom of NOV. NOV(P) at pH 7 provided two H-bonds (see also Figure 5A) and the lowest binding free energy change (kcal/mol).

Protonation of NOV, hydrogen bond and binding free energy change

We then focused on the correlation between the binding free energy changes and the number of H-bonds between GLU235 and the N atom of NOV. Three different protonated structures of NOV (R, S and P) were prepared to vary the number of possible H-bonds formed (see Materials and Methods). The predicted pKa value of NOV (pKa = 8.69) suggested that NOV (P) is the dominant conformation in solution. The production MD simulations of the three NOV configurations reached equilibrium by 1 ns. Two H-bonds between GLU235 and the N atom were formed in the case of NOV (P) at pH 7 (Table 4 and Figure 5A). The other conditions showed the formation of only one H-bond (Figure 5B and C).

An approximate correlation was observed between the binding free energy change and the number of H-bonds between GLU235 and the N atom of NOV. NOV (P) at pH 7 exhibited the lowest binding free energy change of ΔG = -46.26 kcal/mol among all nine combinations, three configurations of NOV(R, S and P) and three differently protonated enzymes (Table 5). All three configurations exhibited an increase in the binding free energy change at pH 5. In particular, NOV(P) exhibited the largest increase in the binding free energy change (i.e. $\Delta\Delta G$ = 36.64 kcal/mol) among the three configurations/combinations of NOV (Table 5).

F213I

According to the prediction by PROPKA, the resultant protonation state of the protein including F213I mutation was identical to the wild-type enzyme. The energy calculation showed that the binding free energy change at pH 7 (ΔG = -38.44 kcal/mol) was lower than at pH 5 and 5X (ΔG = -17.36 kcal/mol and -12.14 kcal/mol, respectively).

Discussion

The MD simulations presented herein theoretically corroborated the hypothetical mechanism of a chemical chaperone. The binding free energy change between β-glucosidase and NOV was demonstrated to increase at pH 5. This is in agreement with the proposed mechanism for a chemical chaperone that dissociates from the target protein in the lysosome and leads to the recovery of enzyme activity (Suzuki, 2008). It was suggested that the binding of a natural

Research Article
OPEN ACCESS Freely available online
doi:10.4172/jpb.1000128
JPB/Vol.3 Issue 4

Protonation	Ligand	G_C	G_R	G_L	ΔG	ΔΔG
pH7	NNBV	-9789.57	-9830.74	56.88	-15.72	-
pH5	NNBV	-9623.12	-9660.33	51.67	-14.46	1.26
pH5X	NNBV	-9641.08	-9668.93	51.64	-23.79	-8.07
pH7	NOV(P)	-9806.97	-9808.45	47.73	-46.26	-
pH5	NOV(P)	-9619.59	-9652.92	47.8	-14.46	31.8
pH5X	NOV(P)	-9595.54	-9633.78	47.86	-9.62	36.64
pH7	NOV(R)	-9829.37	-9852.35	50	-27.01	-
pH5	NOV(R)	-9680.33	-9712.39	45.51	-13.45	13.56
pH5X	NOV(R)	-9661.72	-9687.94	45.82	-19.61	7.4
pH7	NOV(S)	-9846.67	-9869.74	47.37	-24.31	-
pH5	NOV(S)	-9656.28	-9679.67	40.21	-16.81	7.5
pH5X	NOV(S)	-9647.41	-9667.32	41.64	-21.73	2.58

Table 5: Binding free energy changes of β-glucosidase and three configurations of NOV in three different protonation states (kcal/mol).

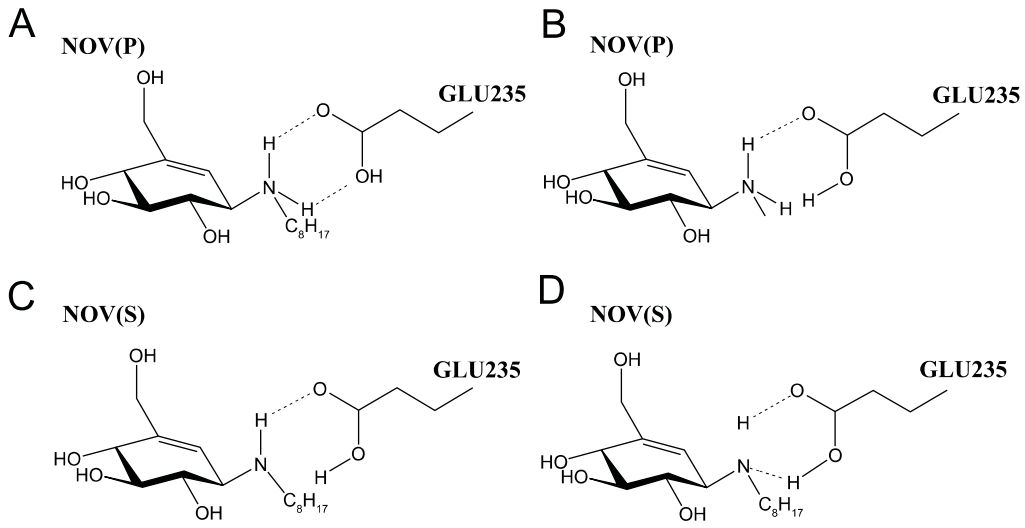

Figure 5: Possible H-bonds between NOVs and the GLU235 residue. (A) Two H-bonds are formed on NOV(P) at pH 7, whereas only one H-bond is formed on NOV(P) at pH 5X (B) and on NOV(S) at pH 7 (C). (D) NOV(S) at pH 5X can provide two H-bonds.

substrate/inhibitor homolog NNBV and the enzyme is almost unchanged or rather tighter at pH 5 than at pH 7. This result does not contradict previous studies on NNOV that showed that NNOV does not function as a chemical chaperone (Lei et al., 2007) but inhibits lysosomal activity (Ogawa et al., 1998). These affinity changes are due to a decrease in the number of H-bonds between the enzyme and NOV primarily caused by the protonation states of the residues ASP127 and GLU235. It has been broadly reported that protonation of a few residues can trigger drastic shifts of the pKa or pH optima of enzymes (Brandsdal et al., 2006; Joshi et al., 2000).

The protonation states of the active residues are influential in the configuration of NOV. Since ASP127 is deprotonated only at pH 7, the hydroxyl groups of NOV show no repulsion towards ASP127 due to unfavorable electrostatic forces. Therefore, deprotonated ASP127 allows deeper binding of NOV into the active site than at pH 5 and 5X. The deeper binding leads to the formation of additional H-bonds between NOV and the enzyme. In particular, the number of the H-bonds between the nucleophile GLU235 and the N atom of NOV were presented to be in correlation with the binding free energy changes. If a ligand of β-glucosidase has an oxygen atom at the position of the N atom, such as glucosylceramide, the O atom can form a H-bond with GLU235 at pH 5X but not at pH 7. Since the O atom is not capable of being protonated, the H-bond can be formed only when GLU235 is protonated i.e. pH 5X in this study. At pH 7, the H-bond cannot be formed because neither GLU235 nor the O atom are protonated. Based on the correlation between the binding free energy changes and the number of H-bonds (Table 4), it is anticipated that the complex of the enzyme and such a ligand without the N atom may exhibit a lower binding free energy change at pH 5X than calculated at pH 7. Namely, the ligand without the aforementioned N atom does not show an affinity decrease in acidic conditions which is required if the ligand is to function as a chemical chaperone. This suggests that the position of the N atom is presumably a crucial factor for NOV to acquire chemical chaperone activity towards β-glucosidase The relative decrease of enzyme-NOV affinity at pH 5 was observed for the F213I mutant and the wild-type structure. The predicted pKa value of each residue in the F213I mutant was calculated to be very similar to the pKa values of the residues of the wild-type protein. The binding free energy changes at pH 5 and 5X were higher than at pH 7. Therefore, we conclude that the mechanism of action of NOV upon the F213I mutant is almost identical to that of the wild-type protein. This result is in

agreement with a previous biochemical study (Lin et al., 2004).

The strategy used here is applicable to other mutations, chaperones and other glycosidases. Although not examined, there are several single-residue mutations of human β-glucosidase, including L444P and N370S. Among these mutants, the enzymatic activity of the L444P mutation is not significantly restored in the presence of NOV (Lin et al, 2004). In addition, the chemical compound N-(n-nonyl) deoxynojirimycin (NN-DNJ) has been shown to increase the activity of the N370S mutant enzyme(Sawkar et al, 2002). Further studies are required to elucidate why NOV does not function as a chemical chaperone with the β-glucosidase L444P mutant. The mechanism of NN-DNJ in rescuing the activity loss caused by the N370S mutation also requires further studies. Apart from β-glucosidase, human α-galactosidase is a feasible target to examine its interaction mechanism with a known chemical chaperone 1-deoxygalactonojirimycin. This is because the 3D structure, detailed kinetic properties and structural stability of several mutants are available for this enzyme(Fan & Ishii, 2007; Garman & Garboczi, 2004; Ishii et al, 2007). We believe that this study presents a MD simulation strategy for understanding the mechanisms of action of chemical chaperones on lysosomal storage diseases.

Although we have described the action mechanism of a chemical chaperone which binds to an enzyme at pH 7 and dissociates at pH 5, there remains a number of questions to answer, including how chemical chaperones improve protein folding stability during the transport process. To fully understand the roles of chemical chaperones from the ER to the lysosome, molecular mechanisms of folding stabilization during transport requires further investigation. Recently, several approaches have been proposed to extract 'collective dynamics' or 'essential dynamics' of proteins from MD trajectories using principal component analysis (Berendsen and Hayward, 2000; Kitao and Go, 1999). Such approaches have been employed to evaluate folding stability (Creveld et al., 1998; Kazmirski et al., 1999). It is noteworthy to apply the collective approaches to glycosidases to elucidate how the chemical chaperones stabilize folding of the enzymes during the transport process, which consequently rescues the enzymes from degradation prior to localization in lysosomes.

In conclusion, the MD simulations results strongly support that residue protonation states at low pH values force dissociation of NOV from the β-glucosidase in the lysosome. Consequently, the hypothesis describing the mechanism of action of NOV was theoretically corroborated.

Acknowledgments

This research was supported by grants from the Ministry of Health, Labour and Welfare of Japan (H14-Kokoro-General-016, H17-Kokoro-General-019, H20-Kokoro-General-022) and a Grant program for bioinformatics research and development of the Japan Science and Technology Agency. Part of the MD calculations was performed using the Research Center for Computational Science, Okazaki, Japan.

References

1. Amaral O, Marcao A, Sa Miranda M, Desnick RJ, Grace ME (2000) Gaucher disease: expression and characterization of mild and severe acid β-glucosidase mutations in Portuguese type 1 patients. Eur J Hum Genet 8: 95-102. » CrossRef » PubMed » Google Scholar
2. Bas DC, Rogers DM, Jensen JH (2008) Very fast prediction and rationalization of pKa values for protein-ligand complexes. Proteins 73: 765-783. » CrossRef » PubMed » Google Scholar
3. Berendsen HJ, Hayward S (2000) Collective protein dynamics in relation to function. Curr Opin Struct Biol 10: 165-169. » CrossRef » PubMed » Google Scholar
4. Boustany RM, Qian WH, Suzuki K (1993) Mutations in acid β-galactosidase cause GM1-gangliosidosis in American patients. Am J Hum Genet 53: 881-888. » CrossRef » PubMed » Google Scholar
5. Brandsdal BO, Smalas AO, Aqvist J (2006) Free energy calculations show that acidic P1 variants undergo large pKa shifts upon binding to trypsin. Proteins 64: 740-748. » CrossRef » PubMed » Google Scholar
6. Case DA, Cheatham TE 3rd, Darden T, Gohlke H, Luo R, et al. (2005) The Amber biomolecular simulation programs. J Comput Chem 26: 1668-1688. » CrossRef » PubMed » Google Scholar
7. Case DA, Darden TA, Cheatham TE III, Simmerling CL, Wang J, et al. (2006) AMBER 9: University of California, San Francisco. » CrossRef » PubMed » Google Scholar
8. Creveld LD, Amadei A, van Schaik RC, Pepermans HA, de Vlieg J, et al. (1998) Identification of functional and unfolding motions of cutinase as obtained from molecular dynamics computer simulations. Proteins 33: 253-264. » CrossRef » PubMed » Google Scholar
9. Davies JP, Eng CM, Hill JA, Malcolm S, MacDermot K, et al. (1996) Fabry disease: fourteen α-galactosidase A mutations in unrelated families from the United Kingdom and other European countries. Eur J Hum Genet 4: 219-224. » CrossRef » PubMed » Google Scholar
10. Essmann U, Perera L, Berkowitz ML, Darden T, Lee H, et al. (1995) A Smooth Particle Mesh Ewald Method. J Chem Phys 103: 8577-8593. » CrossRef » PubMed » Google Scholar
11. Fabrega S, Durand P, Codogno P, Bauvy C, Delomenie C, et al. (2000) Human glucocerebrosidase: heterologous expression of active site mutants in murine null cells. Glycobiology 10: 1217-1224. » CrossRef » PubMed » Google Scholar
12. Fan JQ, Ishii S (2007) Active-site-specific chaperone therapy for Fabry disease. Yin and Yang of enzyme inhibitors. FEBS J 274: 4962-4971. » CrossRef » PubMed » Google Scholar
13. Fan JQ, Ishii S, Asano N, Suzuki Y (1999) Accelerated transport and maturation of lysosomal α-galactosidase A in Fabry lymphoblasts by an enzyme inhibitor. Nat Med 5: 112-115. » CrossRef » PubMed » Google Scholar
14. Garman SC, Garboczi DN (2004) The molecular defect leading to Fabry disease: structure of human á-galactosidase. J Mol Biol 337: 319-335. » CrossRef » PubMed » Google Scholar
15. Ishii S, Chang HH, Kawasaki K, Yasuda K, Wu HL, et al. (2007) Mutant á-galactosidase A enzymes identified in Fabry disease patients with residual enzyme activity: biochemical characterization and restoration of normal intracellular processing by 1-deoxygalactonojirimycin. Biochem J 406: 285-295. » CrossRef » PubMed » Google Scholar
16. Joshi MD, Sidhu G, Pot I, Brayer GD, Withers SG, et al. (2000) Hydrogen bonding and catalysis: a novel explanation for how a single amino acid substitution can change the pH optimum of a glycosidase. J Mol Biol 299: 255-279. » CrossRef » PubMed » Google Scholar
17. Kazmirski SL, Li A, Daggett V (1999) Analysis methods for comparison of multiple molecular dynamics trajectories: applications to protein unfolding pathways and denatured ensembles. J Mol Biol 290: 283-304. » CrossRef » PubMed » Google Scholar
18. Kieseritzky G, Morra G, Knapp EW (2006) Stability and fluctuations of amide hydrogen bonds in a bacterial cytochrome c: a molecular dynamics study. J Biol Inorg Chem 11: 26-40. » CrossRef » PubMed » Google Scholar
19. Kitao A, Go N (1999) Investigating protein dynamics in collective coordinate space. Curr Opin Struct Biol 9: 164-169. » CrossRef » PubMed » Google Scholar
20. Leandro P, Gomes CM (2008) Protein misfolding in conformational disorders: rescue of folding defects and chemical chaperoning. Mini Rev Med Chem 8: 901-911. » CrossRef » PubMed » Google Scholar
21. Lei K, Ninomiya H, Suzuki M, Inoue T, Sawa M, et al. (2007) Enzyme enhancement activity of N-octyl-β-valienamine on β-glucosidase mutants associated with Gaucher disease. Biochim Biophys Acta 1772: 587-596. » CrossRef » PubMed » Google Scholar

Research Article
OPEN ACCESS Freely available online
doi:10.4172/jpb.1000128
JPB/Vol.3 Issue 4

22. Li H, Robertson AD, Jensen JH (2005) Very fast empirical prediction and rationalization of protein pKa values. Proteins 61: 704-721. » CrossRef » PubMed » Google Scholar

23. Lieberman RL, Wustman BA, Huertas P, Powe AC Jr, Pine CW, et al. (2007) Structure of acid β-glucosidase with pharmacological chaperone provides insight into Gaucher disease. Nat Chem Biol 3: 101-107. » CrossRef » PubMed » Google Scholar

24. Lin H, Sugimoto Y, Ohsaki Y, Ninomiya H, Oka A, et al. (2004) N-octyl-β-valienamine up-regulates activity of F213I mutant beta-glucosidase in cultured cells: a potential chemical chaperone therapy for Gaucher disease. Biochim Biophys Acta 1689: 219-228. » CrossRef » PubMed » Google Scholar

25. Matsuda J, Suzuki O, Oshima A, Yamamoto Y, Noguchi A, et al. (2003) Chemical chaperone therapy for brain pathology in GM1-gangliosidosis. Proc Natl Acad Sci USA 100: 15912-15917. » CrossRef » PubMed » Google Scholar

26. Miao S, McCarter JD, Grace ME, Grabowski GA, Aebersold R, et al. (1994) Identification of Glu340 as the active-site nucleophile in human glucocerebrosidase by use of electrospray tandem mass spectrometry. J Biol Chem 269: 10975-10978. » CrossRef » PubMed » Google Scholar

27. Ogawa S, Ashiura M, Uchida C, Watanabe S, Yamazaki C, et al. (1996) Synthesis of potent β-D-glucocerebrosidase inhibitors: N-alkyl-β-valienamines. Bioorg Med Chem Lett 6: 929-932. » CrossRef » PubMed » Google Scholar

28. Ogawa S, Kobayashi Y, Kabayama K, Jimbo M, Inokuchi J (1998) Chemical modification of betaglucocerebrosidase inhibitor N-octyl-beta-valienamine: synthesis and biological evaluation of N-alkanoyl and N-alkyl derivatives. Bioorg Med Chem 6: 1955-1962. » CrossRef » PubMed » Google Scholar

29. Okumiya T, Ishii S, Kase R, Kamei S, Sakuraba H, et al. (1995a) β-galactosidase gene mutations in Fabry disease: heterogeneous expressions of mutant enzyme proteins. Hum Genet 95: 557-561. » CrossRef » PubMed » Google Scholar

30. Okumiya T, Ishii S, Takenaka T, Kase R, Kamei S, et al. (1995b) Galactose stabilizes various missense mutants of α-galactosidase in Fabry disease. Biochem Biophys Res Commun 214: 1219-1224. » CrossRef » PubMed » Google Scholar

31. Perlmutter DH (2002) Chemical chaperones: a pharmacological strategy for disorders of protein folding and trafficking. Pediatr Res 52: 832-836. » CrossRef » PubMed » Google Scholar

32. Pettersen EF, Goddard TD, Huang CC, Couch GS, Greenblatt DM, et al. (2004) UCSF Chimera—a visualization system for exploratory research and analysis. J Comput Chem 25: 1605-1612. » CrossRef » PubMed » Google Scholar

33. Premkumar L, Sawkar AR, Boldin-Adamsky S, Toker L, Silman I, et al. (2005) X-ray structure of human acid-β-glucosidase covalently bound to conduritol-B-epoxide. Implications for Gaucher disease. J Biol Chem 280: 23815-23819. » CrossRef » PubMed » Google Scholar

34. Rodziewicz-Motowidlo S, Wahlbom M, Wang X, Lagiewka J, Janowski R, et al. (2006) Checking the conformational stability of cystatin C and its L68Q variant by molecular dynamics studies: why is the L68Q variant amyloidogenic? J Struct Biol 154: 68-78. » CrossRef » PubMed » Google Scholar

35. Ryckaert JP, Ciccotti G, Berendsen HJC (1977) Numerical integration of the cartesian equations of motion of a system with constraints: molecular dynamics of n-alkanes. J Comput Phys 23: 327-341. » CrossRef » PubMed » Google Scholar

36. Sawkar AR, Cheng WC, Beutler E, Wong CH, Balch WE, et al. (2002) Chemical chaperones increase the cellular activity of N370S beta-glucosidase: a therapeutic strategy for Gaucher disease. Proc Natl Acad Sci USA 99: 15428-15433. » CrossRef » PubMed » Google Scholar

37. Suzuki Y (2006) β-galactosidase deficiency: an approach to chaperone therapy. J Inherit Metab Dis 29: 471-476. » CrossRef » PubMed » Google Scholar

38. Suzuki Y (2008) Chemical chaperone therapy for GM1-gangliosidosis. Cell Mol Life Sci 65: 351-353. » CrossRef » PubMed » Google Scholar

39. Suzuki Y, Ichinomiya S, Kurosawa M, Ohkubo M, Watanabe H, et al. (2007) Chemical chaperone therapy: clinical effect in murine GM1-gangliosidosis. Ann Neurol 62: 671-675. » CrossRef » PubMed » Google Scholar

40. Swanson JM, Henchman RH, McCammon JA (2004) Revisiting free energy calculations: a theoretical connection to MM/PBSA and direct calculation of the association free energy. Biophys J 86: 67-74. » CrossRef » PubMed » Google Scholar

41. Yam GH, Zuber C, Roth J (2005) A synthetic chaperone corrects the trafficking defect and disease phenotype in a protein misfolding disorder. FASEB J 19: 12-18. » CrossRef » PubMed » Google Scholar